ORIGINAL PAPER

Development of a medium/long-haul reference aircraft

Benjamin M. H. J. Fröhler[1] · **Jannik Häßy**[2] · **Mohammad Abu-Zurayk**[3]

Abstract

For the evaluation of future aircraft architectures or novel technologies, a well-understood and sound reference to compare to is essential to prove the impact of intended changes. A reference aircraft serves as a basis for calibration of the aircraft and is used as a starting point for subsequent investigations, sensitivity studies or optimizations. The prime need for such a reference arose from the European Clean-Sky-2 project HLFC-Win (Hybrid Laminar Flow Control—Wing), where no industrial reference data for a conventional aircraft were available. The project investigates a HLFC system integrated into the wing aiming to reduce the wing drag and consequently reducing the fuel consumption. Therefore, this paper presents the D300-XRF1 designed by DLR, which is based on the AIRBUS research aircraft XRF1 (eXternal Research Forum). It is intended to be used as a reference aircraft database representing aircraft for medium- and long-range missions. A variable fidelity multidisciplinary design analysis and optimization (MDAO) aircraft design environment is set up to provide a consistent estimate of the geometry, mass breakdown, propulsion system, aerodynamics and aircraft performance. A conceptual aircraft design tool is utilized in the aircraft design environment to initialize the process, and higher-fidelity modules are used to enhance the results. The presented results describe the overall aircraft characteristics of the D300-XRF1 based on 2010 entry into service technology level and is offered to be used as a reference within the aviation research community, hopefully reducing similar design efforts in other research projects.The aircraft operates at a design cruise Mach number of 0.83, has a design range of 5500 NM and transports a payload of 31.5 t (300 PAX at 105 kg/PAX). The D300-XRF1 serves as a consistent reference aircraft database and provides a holistic overview of the aircraft's performance that has been presented to and approved by AIRBUS. Therefore, this reference aircraft design can be used for future studies and to assess new technologies on a sophisticated level.

Abbreviations

A/C	Aircraft
AEO	All engine operating
AF	Airframe
AMC	Aircraft mission calculator
APP	Approach
APU	Auxiliary power unit
ASK	Available seat kilometers
ATC	Air traffic control
BFL	Balanced field length
BPR	Bypass Ratio
CAD	Computer-aided design
CAS	Calibrated airspeed
CFD	Computational fluid dynamics
CFRP	Carbon fiber-reinforced polymers
CPACS	Common parametric aircraft configuration schema
CR	Cruise
CS-25	Certification specifications for large aero-planes
DLR	German aerospace center
DOC	Direct operating costs

✉ Benjamin M. H. J. Fröhler
   Benjamin.Froehler@dlr.de

   Jannik Häßy
   Jannik.Haessy@dlr.de

   Mohammad Abu-Zurayk
   Mohammed.Abu-Zurayk@dlr.de

1 Institute of System Architectures in Aeronautics, German Aerospace Center, Hein-Sass-Weg 22, 21129 Hamburg, Germany

2 Institute of Propulsion Technology, German Aerospace Center, Linder Höhe, 51147 Köln, Germany

3 Institute of Aerodynamics and Flow Technology, German Aerospace Center, Lilienthalplatz 7, 38108 Braunschweig, Germany

EIS	Entry into service
EOF	End of field
FL	Flight level
FS	Front spar
GLA	Gust load alleviation
GTlab	Gas turbine laboratory
HB	HandbookAero
h	Altitude
HiFi	High fidelity
HLFC	Hybrid laminar flow control
HTP	Horizontal tail plane
ICA	Initial cruise altitude
ISA	International standard atmosphere
LE	Leading edge
LFL	Landing field length
LiLi	Lifting-line
LoFi	Low fidelity
LOF	Lift-off
LPA	Large passenger aircraft
MCL	Maximum climb thrust rating
MCR	Maximum cruise thrust rating
MDAO	Multidisciplinary design analysis and optimization
MEM	Manufacturer empty mass
MLA	Maneuver load alleviation
MLM	Maximum landing mass
M	Mach number
MTOM	Maximum take-off mass
MTO	Maximum take-off thrust rating
MZFM	Maximum zero-fuel mass
OAD	Overall aircraft design
OEI	One-engine inoperative
OEM	Operating empty mass
OPR	Overall pressure ratio
PAX	Passenger
RCE	Remote component environment
ROC	Rate of climb
RS	Rear spar
RTO	Rejected take-off
RWY	Runway
SFC	Specific fuel consumption
SL	Sea level
S	Reference area
TE	Trailing edge
TLARs	Top-level aircraft requirements
TOC	Top of climb
TOD	Take-off distance
TOFL	Take-off field length
TOM	Take-off mass
tSFC	Thrust-specific fuel consumption
VTP	Vertical tail plane
XRF1	EXternal research forum

1 Introduction

Quantitative assessment of futuristic aircraft architectures or novel technologies is particularly challenging due to the highly multidisciplinary nature of aircraft and the inclusion of multi-fidelity simulation results. A reference aircraft is used as a basis to calibrate the applied methods and to determine the overall system behavior from the modeled aircraft. A reliable assessment of new technologies is only possible when the reference aircraft itself is consistent. This include all involved disciplines, which provide data for, e.g., aerodynamics, engine performance or masses. Consortiums within aerospace research projects define reference configurations, but the data are limited, because (industrial) partners share data only by need-to-know principle. In addition, a standardized reference aircraft allows a comparison of research projects and would enable a sophisticated assessment of different technologies due to a high level of consistency within the aircraft design. Therefore, AIRBUS provided the XRF1 (eXternal Research Forum) test case as research configuration of a long-range aircraft for demonstration of new technologies. The XRF1 is an industry standard multidisciplinary test case, representing a typical long-haul wide body aircraft. The XRF1 has already been used in multiple European and international projects; however, some holistic aircraft design data were not available and an overall aircraft assessment not possible. The German Aerospace Center (DLR) created a design based on the XRF1 to provide an overall and consistent aircraft definition.

The current paper will provide an overview of the overall aircraft design (OAD) process and will describe the used and developed methods. Finally, based on the introduced methods, results are presented for the DLR design of the new aircraft configuration. The new reference aircraft designed by DLR will be referred to as the "D300-XRF1".

2 Overview of past XRF1 projects

Various projects used the XRF1 as a basis to analyze and optimize different disciplines of the aircraft. A majority of work has been done on optimizing the wing and its high-speed aerodynamics, however, the OAD was often not considered. This reduces the quality of the overall assessment of the wing optimization, as aircraft designs are highly multidisciplinary, e.g., by changing the wing position, the empennage needs to be modified as well. Furthermore, such a design modification causes snow-ball effects, because masses and centers of gravity are changing, which needs to be considered.

Remarkable work has been done using the XRF1 within many international projects, just to name a few: The project ARTEMIS initially developed the XRF1 in which a combination of a high-fidelity aero-structure optimization with a low-fidelity overall aircraft optimization was applied [1]. The project AFLONEXT is aiming at proving and maturing highly promising flow control technologies for novel aircraft configurations to achieve a quantum leap in improving aircraft's performance [2]. Within the project MADELEINE, an adjunct-based multidisciplinary optimization using high-precision numerical method is developed to analyze the XRF1 [3]. The project SFWA focuses on wing technologies by using a passive load reduction by means of aeroelastic tailoring and active methods for load reduction and in addition, creating a design process and solutions for aircraft wings giving optimal response with respect to loads, comfort and performance [4, 5]. The project AEROGUST focused on producing a more accurate simulation-based gust load process using reduced order models. As the current approach lies on expensive high-fidelity computation or wind tunnel test, industry is relying on model to accurate and fast model for designing of aircraft. Gust loads often define the maximum load on an aircraft wing and more reliable predictions of these gust loads could reduce structural weight and thus fuel consumption of the aircraft [6].

Most data were available by projects with DLR involvement. Especially the project Digital-X established a fast, multidisciplinary design process at a preliminary design stage. The design process is used for the first optimization of the overall aircraft configuration with interfaces to results of higher-fidelity methods. The Digital-X project developed and enhanced these tools and used the XRF1 configuration as reference [7].

The succeeding project, namely the VicToria project [8], analyzed numerical methods for the overall aircraft design and for the full description of the physical properties of aircraft. The main goal, in which the XRF1 was used as a test case, was to further develop and improve a gradient based aero-structural optimization of a full aircraft configuration for a limited number of test cases. A cross-discipline team combining aerodynamics, structure, loads, aeroelasticity, propulsion and overall aircraft design improved the optimization chain within the project. The results of the optimization chain are the aerodynamic performance using high-fidelity CFD, aircraft performance in low fidelity, loads and structural analysis with FEM and an engine design [8–10].

The project Con.Move: Nekon [11] aims to determine the load hierarchy of weight potential of load reduction systems, the identification of interaction between structural deformation (aeroelastic tailoring) and active load alleviation systems (MLA/GLA) and the investigation into multi-functional control surfaces. As part of the project, a reference XRF1 configuration was designed by the multidisciplinary integrated conceptual aircraft design and optimization environment MICADO [12]. An overall aircraft design was developed with key aircraft characteristics, the general geometry and planform, engine characteristics, mass breakdown, aerodynamics and performances [13]. A full three-dimensional design of the XRF1 high lift and wing movables arrangement is developed and the take-off and landing configuration is defined. Part of the development is a CAD model with fully extendable slats, flaps and ailerons and CFD computation of polar to verify the high lift performance [14].

Two main projects were identified to provide the necessary OAD dependencies, the DLR project VicToria [8] and the LuFo project Con.Move: Nekon [11]. Many subsequent projects are based on these two projects which provided most consistent data for the design.

3 Multidisciplinary aircraft design environment

When designing an aircraft or evaluating a new technology, it is important to have a reference aircraft that is based on the same methods and assumptions as the new design for a proper comparison. A Multidisciplinary Design Analysis and Optimization (MDAO) aircraft design environment was created for the design of the D300-XRF1, capable of describing the reference aircraft as previously specified or providing an estimate of how technological improvements will impact the aircraft design. This chapter describes the MDAO aircraft design environment and each disciplinary module to understand the methods used and the assumptions underlying the design.

To integrate and combine several tools on conceptual aircraft design level as well as on higher-fidelity disciplinary level, the workflow-driven integration platform RCE (Remote Component Environment) [15] is used. Within this MDAO aircraft design environment, the sub-processes communicate though their inputs and outputs in a common language. The air vehicles are defined using the data definition named "Common Parametric Aircraft Configuration Schema" (CPACS) [16], which supports the exchange information and stores data of aircraft characteristics.

The design process of the D300-XRF1 is described in Fig. 1 as a flowchart. At the beginning of the aircraft design process, the top-level aircraft requirements (TLARs) and other design parameter are defined. The design parameters contain further details about the geometry and project specific settings as well as general settings for the tools used. These information are translated for the conceptual aircraft design tool openAD [17], which is based on handbook methods [18–23] and is extended by
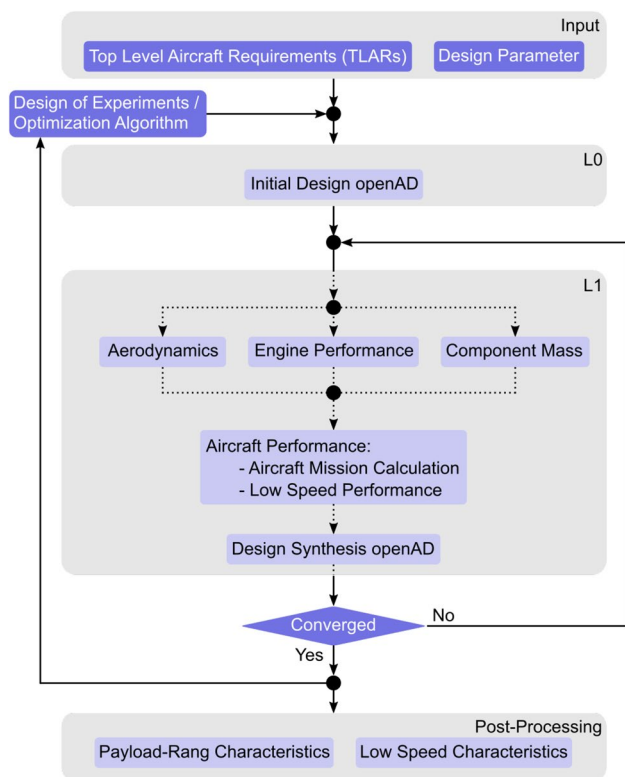
Fig. 1 MDAO conceptual aircraft design environment

in-house methods. OpenAD is a level-0 conceptual aircraft design tool to initialize the OAD process and obtain a geometry definition and a first aircraft performance estimate. Higher-fidelity disciplinary tools are allocated in the level-1 domain, which refine the preliminary results of openAD. The design of the D300-XRF1 included refinements in: aerodynamics, engine performance, detailed mass breakdown and aircraft performance. Subsequently, the results of the higher fidelity discipline tools are fed back into openAD for the synthesis. To achieve a consistent aircraft design, a residual of less than 1e-4 must be maintained for the final two iterations. The process is iterated until the maximum take-off mass (MTOM), operating empty mass (OEM), wing position, empennage lever arm, and mid-cruise aerodynamics converge. Once consistency is achieved, additional information about payload-range characteristics or balanced field length calculations can be provided in a post-processing step.

As described before, the level-1 domain is dedicated for refinements of the openAD results. The level-1 methods are based on simplified physics and used semi-analytical or simple numerical calculations. Since these methods are based on simplification, a prior calibration step (see Sect. 4) using the HiFi data from the two DLR internal projects is necessary. In the following, the disciplinary tools are introduced.

3.1 Aerodynamic module

The aerodynamic forces, i.e., lift, pitching moment, induced drag, viscous drag, and wave drag, are estimated for the entire flight envelope using two tools, namely: Lifting-Line (LiLi) and HandbookAero (HB). LiLi [24] is based on the potential flow theory, assuming an inviscid, irrotational and steady flow around a wing following the theory of the thin airfoil and with an extension to subsonic flow. The primary objective of LiLi, in the scope of the conceptual design, is the estimation of lift, induced drag and pitching moment of non-planar wings within the flight envelope. In addition to LiLi, HB is used as a second aerodynamic tool to approximate viscous drag for each component separately. HB estimates the viscous drag by empirical and semi-empirical methods [18, 21] and can be extended by user-defined equations. Both tools have a CPACS input and output interface for straightforward integration to RCE. The wave drag is calculated in an external python script with a dependency on the Mach number, wing geometry and lift coefficient [18, 19].

3.2 Propulsion system module

The engine performance is divided into a previous development of the engine model and the integration of the engine model into the OAD process. The virtual engine platform GTlab (Gas Turbine Laboratory) [25] is a framework for the preliminary aircraft engine design. Within the framework, different modules are included and offer an engine geometry library of each component, a thermodynamic cycle design, an aerodynamic design of the main internal engine components, structural characteristics of both blades and disks as well as a detailed mass breakdown. The conceptual aircraft design provides engine requirements such as thrust and offtakes for different operating conditions and engine ratings. Based on the engine requirements, an engine concept is defined and the analysis provides overall performance data for the entire flight envelope considering the design point and the off-design to ensure that operating limits are maintained. For further collaboration between the engine design and the overall aircraft design, the engine model provides a CPACS output, which is imported to the OAD process.

3.3 Component mass module

To estimate the mass of primary and secondary wing structure, a method presented by TORENBEEK [19] is used. The implemented method is based on a wing box sizing principle applying statistics for 1-g stress levels. Classical beam theory is used to estimate the primary wing structure, applying an analytic integration along the span of the material that must resist bending and shear. Material specific allowances

for stiffness are prescribed to handle aeroelasticity and reduced stress levels to increase service life. The secondary structure, i.e., control surfaces, attachments and supports are approximated by a semi-empirical analysis and scaled based on MTOM as presented in [19]. The tool is CPACS native and interprets the necessary aircraft data and provides an extended wing mass breakdown.

3.4 Aircraft performance module

Two tools, LSperfo and AMC, are used to evaluate the performance of the aircraft. The results of the preceding aerodynamics and engine performance calculations are transmitted to the two aircraft performance tools. LSperfo [26] is performing the low-speed performance calculation for take-off as well as the approach & landing. Throughout the level-1 segment of the OAD process, LSperfo analyses the trajectories for the All Engine Operating (AEO) condition. A standard take-off trajectory (see Fig. 16) and landing trajectory (see Fig. 19) are defined by the AIRBUS manual [27]. The take-off phase is divided into take-off distance and take-off flight path in which different aircraft configurations and settings are prescribed. For the landing phase, an approach and a landing distance segment are applied. From the take-off as well as the approach & landing calculations, the fuel consumption is extracted and transmitted to the Aircraft Mission Calculator (AMC) [17]. The tool AMC uses fuel fractions for the taxiing, take-off as well as the approach & landing phase. AMC estimates high-speed performance by solving the 2D total motion equations and analyzing the climb, cruise, and descent phases with a clean wing configuration, i.e., the control surfaces are retraced. An optimization of the initial cruise altitude is performed and during the cruise phase, a combination of constant altitude with a step-climb is applied. The position of the step is depending on the specific range, which considers the aerodynamic and engine performance. The two aircraft performance tools are deployed again for the post-processing of the OAD process to provide more information on the aircraft design, i.e., payload-range characteristics or balanced field length characteristics and sensitivities on take-off/ landing field length.

4 Aircraft design assumptions and model calibration

Several assumptions were made for the design of the reference aircraft. Listed below are the assumed technology status of the components with its entry into service (EIS) and the aircraft design concept.

- Technology status:
  - Airframe: 1995 (Aluminum alloys material assumed)
  - Wing: 2010 (Improved aluminum alloys technologies compared to A330-300 with EIS 1994)
  - Engine: 2010 (Matching of engine to BPR and SFC)
- Single point design:
  - Family concept is not considered
  - Max. fuel is derived from payload-range characteristics [28] with fixed volume
- Aerodynamic performance:
  - HiFi aerodynamic results [8] are used for calibration of LoFi aerodynamics
  - No winglets are used for the aircraft design
  - Potential for aerodynamic efficiency increase
- Material technology:
  - Mixture of aluminum 2024 and aluminum 7075 [8]
- Operating items:
  - Typical 3 class layout of an airline cabin mass definition

In conceptual aircraft design, empirical and semi-empirical methods are used to achieve a fast assessment of the aircraft. However, these simplified methods are not without error and a calibration to a known reference is crucial. For the D300-XRF1, calibrations were based on the results of VicToria [8] and Con.Move: Nekon [11] project. The project VicToria provided a detailed mass breakdown, geometry definition and HiFi aerodynamic performance data. Additionally, the project ConMove: Nekon [11] provided information on the low-speed performance and a detailed description of the moveable arrangement.
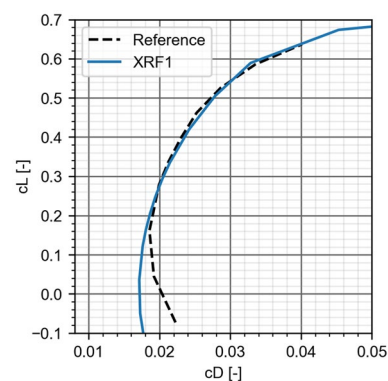

Fig. 2 Calibrated drag polar of the D300-XRF1 compared to HiFi CFD results at a Mach number of 0.83 and FL330

The aerodynamics are calibrated in terms of zero lift drag and lift depended pressure drag to match the HiFi CFD results. In addition to the model calibration, drag factors are applied to account for further components, which are not in the model. The belly fairing is added to the fuselage and assigned a factor of 1.1 to the zero lift drag of the wing. Figure 2 depict the final aerodynamic polar of the D300-XRF1 compared to the HiFi CFD results at cruise condition with a Mach number of 0.83 and a flight level (FL) FL330.

Table 1 Top-level aircraft requirements (TLARs) [28]

| Parameter	Unit	Value
Technology status airframe	Year	1995
Technology status wing and engine	Year	2010
Design range	NM	5500
Study mission range	NM	3000
Design cruise mach number	–	0.83
Initial cruise altitude	ft	33000
Service ceiling	ft	43000
Take-off balanced field length (SL, ISA)	m	⩽2800
Landing field length (MLM, SL, ISA, Dry RWY)	m	⩽2250
Max. operating mach number (MMO)	–	0.87
Max. operating speed (V_{MO})	kn	340
Climb speed (calibrated airspeed)	kn	300
Descent speed (calibrated airspeed)	kn	250
Approach speed (calibrated airspeed)	kn	$121 \leqslant V_{APP} \leqslant 141$
Number of passengers (3 class standard layout)	–	300
Design mission payload (105 kg/PAX)	t	31.5
Study mission payload (105 kg/PAX)	t	25.2
Max payload	t	48
ICAO aerodrome reference code	–	ICAO category E

5 D300-XRF1 reference aircraft

D300-XRF1 is based on the same TLARs as the AIRBUS XRF1 [28] and is listed in Table 1. The technology status of the airframe as well as the wing and the engine assume a different year for entry into service to comply with the prescribed component masses. For the mission, two ranges are analyzed, i.e., the design mission and a study mission with a range of 5500 NM and 3000 NM, respectively. The aircraft operates at a design cruise Mach number of 0.83 with an initial cruise altitude (ICA) of 33000 ft and a ceiling altitude of 43000 ft. A design mission with a range of 5500 NM and a number of passengers of 300 PAX at 105 kg/PAX was defined according to the AIRBUS [28]. For this design mission, all performance data are calibrated, i.e., engine, aerodynamic performances as well as the mass breakdown.

5.1 Geometry

The three-view of the D300-XRF1 is shown in Fig. 3 (detailed three-view in the Appendix A, Fig. 25) and was derived from the CAD model and transmitted to CPACS using the conceptual aircraft design tool openAD [17] and a simplified geometry. The simplification is necessary to adapt the input to openAD, but since the HiFi aerodynamics calculations used the detailed CAD geometry, there is no significant reduction in fidelity in estimating aircraft performance. The wing was modeled according to the jig-shape as a five-station wing without winglets and resulted to a reference area of $S = 374.55$ m^2. The volume coefficient of the vertical and horizontal tail plane resulted from its reference area and the lever arm of the empennage. Moreover, the rear- and side clearance angle are estimated to be 10.7° and 11°, respectively, which exceeded the minimum required clearance.
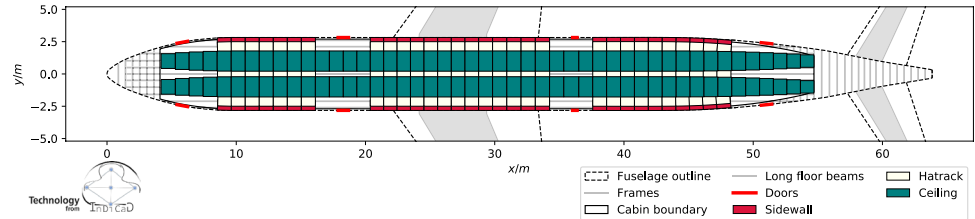
Fig. 3 CPACS three-view
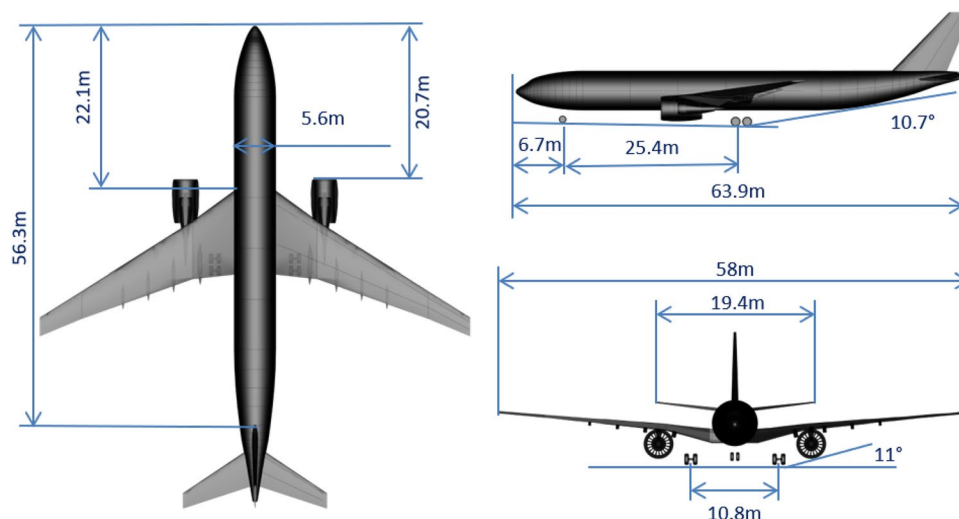
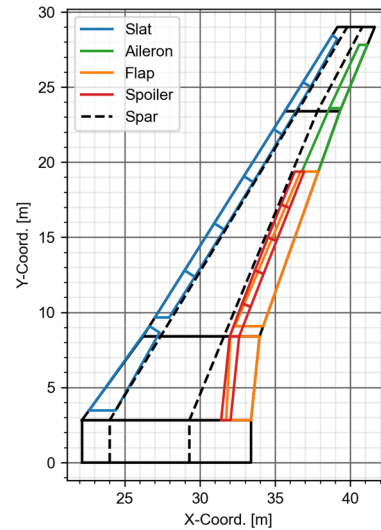**Fig. 4** Three class, twin-aisle cabin layout of the D300-XRF1 [29]
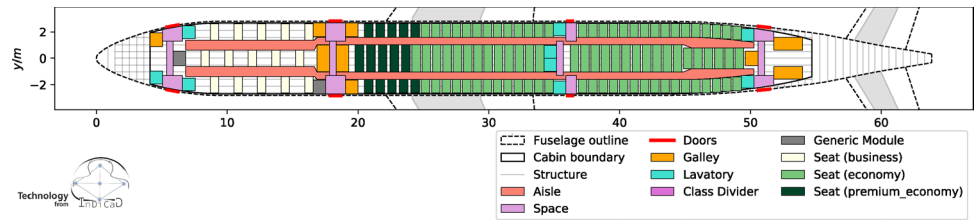
Fig. 5 Paneling element placement considering cabin boundary and frame positions of the D300-XRF1 [29]

Table 2 Cabin layout definition of the D300-XRF1

Parameter	Value
Max passengers	300
Cabin layout:	3 Class
Business class	30 Seats
Premium economy class	40 Seats
Economy class	230 Seats
Lavatories	9
Galleys	9
Flight crew members	2
Cabin attendants	9
Exit types	AAAIA
Over wing exits	0
Cabin length	50.6 m (pressure bulk-head at VTP-FS)
Cockpit length	4.0 m

Fig. 6 Wing planform with moveable arrangement and spar position

The cabin layout is designed using the DLR in-house tool FuGA [29]. A three class, twin-aisle cabin layout is shown in Fig. 4 is designed for a passenger capacity of 300PAX. The three classes are divided in business, premium economy and economy class. Figure 5 shows the placement of the sidewall panel elements with the position of the hatracks. Table 2 lists the characteristics of the D300-XRF1 cabin. The cabin comprises nine lavatories and nine galleys with two flight crew members and nine cabin attendants. The cockpit length is 4.0 m and the cabin length of 50.6 m resulted from the length between the rear wall of the cockpit and the longitudinal position of the rear pressure bulkhead, which is positioned at the front spar of the VTP. The exit types are defined according to the "Certification Specifications for Large Aeroplanes" (CS-25) [30] with exit types A and types I.

5.2 Wing structure

The wing is defined as a multi-crank wing with five stations and four segments, whereas, the HTP and VTP are defined as single trapezoid surfaces. The wing exhibits a trailing edge as well as a leading edge kink and with an average 1/4 chord sweep of 30°. A total wing reference area of $S = 374.55$ m^2 resulted from the simplification of a five-station wing and together with a span of $b = 58$ m, an aspect ratio of 8.98 is reached. The wing airfoils are standard profiles for transport aircraft [31] and are selected by the conceptual aircraft design tool openAD. The airfoils are scaled in thickness for all defined wing stations, i.e., root, kink, mid and tip, and are linearly interpolated between each other. The overall wing geometry including the moveable arrangement and spar position is shown in Fig. 6. The movable layout was
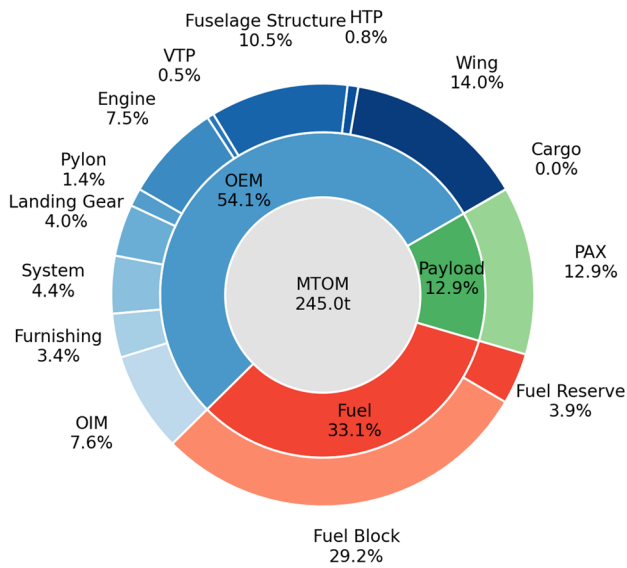
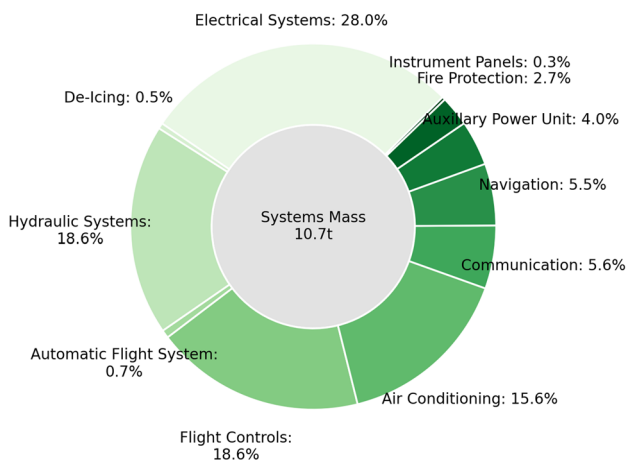**Fig. 7** Overview of the D300-XRF1 mass breakdown

Fig. 9 Overview of the D300-XRF1 full span wing mass breakdown

Fig. 8 Overview of the D300-XRF1 system mass breakdown
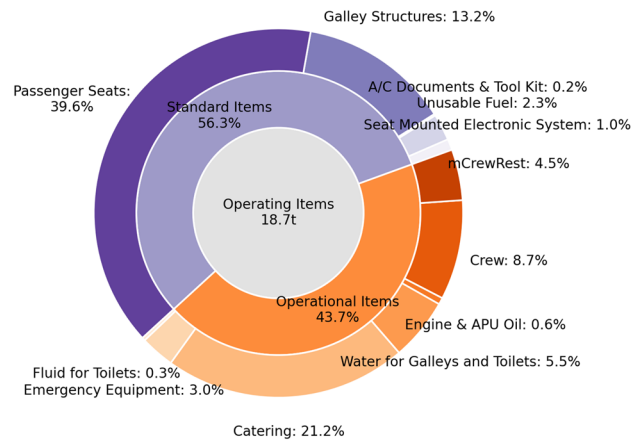
Fig. 10 Overview of the D300-XRF1 operator's items mass breakdown

defined by the project Con.Move: Nekon [11] and is adapted for the standard layout of OpenAD.

5.3 Mass properties

The assumed material composition of the D300-XRF1 is a mixture of the aluminum alloy 2024 and the aluminum alloy 7075 as defined in VicToria [8].

An overview of the overall mass breakdown is shown in Fig. 7 and a detailed description is listed in the Appendix A, Table 8. In addition, the system mass breakdown is shown in Fig. 8 with a detailed description in the Appendix A, Table 9. The MTOM of 245 t is divided into major three parts: payload with 13%, fuel with 33% and operating empty mass with 54%. The component masses are calibrated
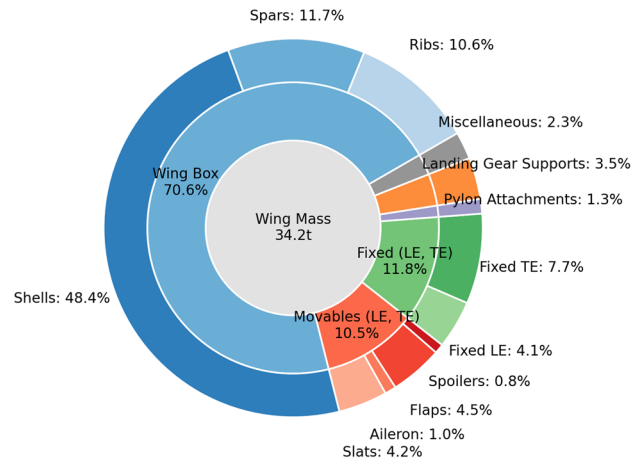
according to the results by the VicToria project [8] and the operator's items are used to calibrate the major aircraft mass, i.e., MTOM, OEM, MLM and MZFM, which reflect a rather heavy operator option configuration.

Additional to the overall mass breakdown, a more detailed breakdown for the full span wing structure is depicted in Fig. 9 (detailed description is listed in the Appendix A in Table 10). The breakdown includes the primary and secondary wing structure. The primary wing structure contributes with the highest proportion of 70.6% and is composed of the ribs, shell and spars. The secondary wing structure consists of the movable arrangement, additional supports and attachments including all additional system masses for controlling the movable arrangement. Miscellaneous items are used to complete the mass breakdown and consists of paint, doors, hatches, etc. The proposed breakdown of the wing mass is obtained using the methods of TORENBEEK [19] and provides

a reasonable starting point for a more detailed analysis of the wing structure, e.g., using finite element methods.

The operator's items mass breakdown is shown in Fig. 10 (detailed description is listed in the Appendix A in Table 11) and are derived for a three-class cabin layout and a long-haul aircraft. The 18.7 t operator's items are divided into standard items with a proportion of 56% and operational items of 44%. The cabin layout with its passenger seats and galley structure adds the largest contribution to the operator's items with a 53% share.

5.4 Aerodynamics

To access the aircraft performance, knowledge of the aerodynamic polars are required. The low-speed and high-speed aerodynamics of the D300-XRF1 are described in the following. Low-speed aerodynamics are provided by openAD [17] which estimates the aerodynamic polar by a LoFi method with deflected control surfaces. For the high-speed aerodynamics, higher-fidelity results were available to calibrate the LoFi results as described in Sect. 4.

Low-speed aerodynamics are important for the assessment of take-off and landing performances. At low speed, the control surfaces are deflected to increase lift by enlarging the wing area and adding camber to the profile. Leading edge slats, trailing edge flaps and ailerons are used to support low-speed aerodynamics. For the D300-XRF1, single slotted Fowler flaps are used. Table 3 lists the control surface deflections for slats, flaps and ailerons during the take-off as well as approach & landing segment. The corresponding aerodynamic polar are depicted in Fig. 11a and b for both flight conditions with a control surface configuration defined in Table 3 and for a Mach number of 0.23 and at an altitude of 400 ft. The respective polars are assigned to the take-off and landing masses of 245 t and 195.2 t, respectively.

The high-speed aerodynamics determine the cruise performance of the D300-XRF1. At high speed, the wing is in clean configuration with all control surfaces retracted. As fuel is consumed, the aerodynamic performances change throughout the mission. Figure 12a and b shows the exemplary aerodynamic polar at mid-cruise condition for the cruise Mach number of 0.83 and at FL350. The polars show a L/D ratio of 17.8 at mid-cruise condition with a lift coefficient of $c_L = 0.476$ and a drag coefficient of $c_D = 0.0268$ and a rapid decline in aerodynamic performance subsequent to the maximum L/D ratio is observed. This behavior indicates the influence of the wave drag on the performance at higher lift coefficients.

In addition to the aerodynamic polar, a detailed drag breakdown at mid-cruise condition is shown in Fig. 13. The total drag of 268 DC is decomposed of zero lift drag, induced drag, wave drag and lift dependent pressure drag. The zero lift drag has the highest contribution on the total drag and is further divided into the zero lift drag of the individual aircraft components that are exposed to the air flow. The fuselage and wing contribute with 24.8% and 22.3% to the zero lift drag. Moreover, the induced drag with its 36.6% contribution to the total drag, indicate a high influence on the aircraft performance. As the D300-XRF1 is modeled

Table 3 Control surface deflection [11]

Parameter	Cruise	Take-off			Landing
Configuration Name	Clean	1	2	3	Full
Definition:	0000	1500	2220	2228	2233
Leading Edge					
Slats:	0	15	22	22	22
Trailing Edge					
Flaps:	0	0	20	28	33
Ailerons:	0	5	5	10	10

Fig. 11 Low-speed aerodynamic polar with control surface configuration defined in Table 3

(a) Drag polar

(b) Lift over drag polar

Fig. 12 High-speed aerodynamic polar

(a) Drag polar
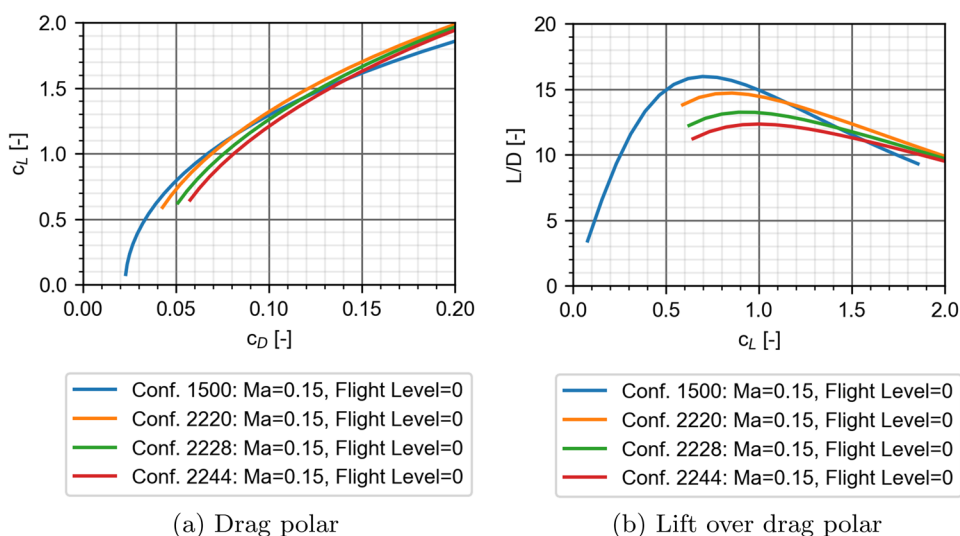
(b) Lift over drag polar
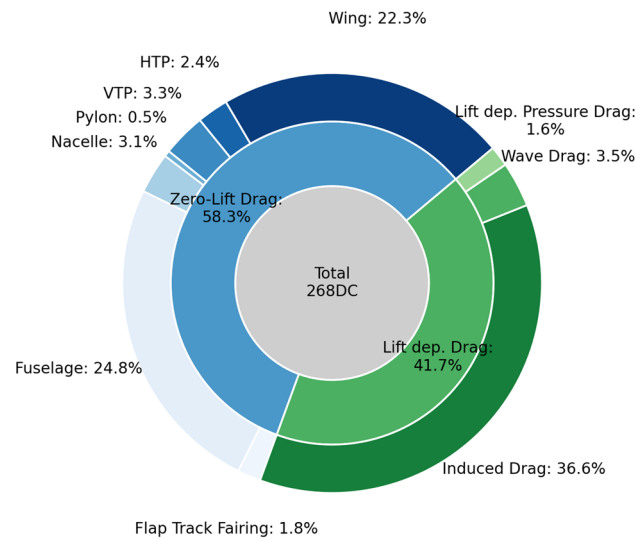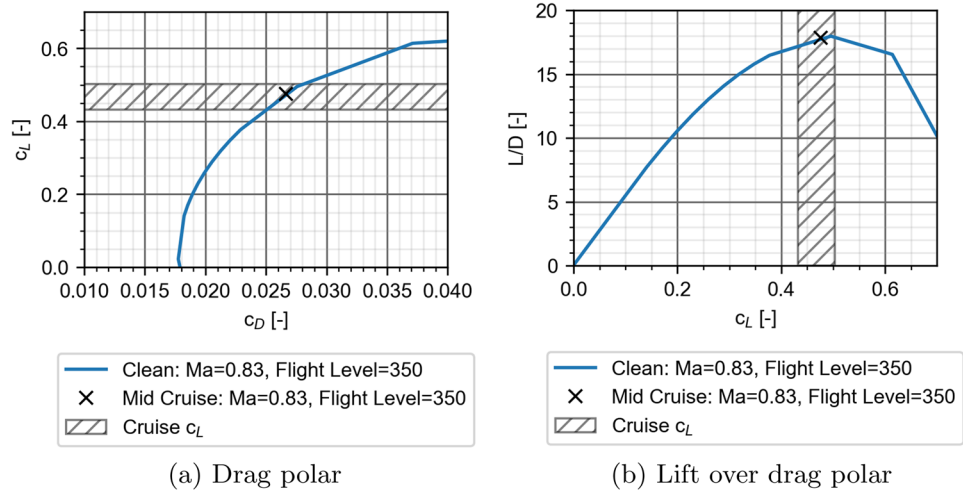
Fig. 13 Drag breakdown at mid-cruise condition (Mach number of 0.83, FL350 and c_L of 0.476)

without wing tip extensions, i.e., winglets, further improvements of the aerodynamic efficiency are possible due to a reduction in induced drag.

5.5 Propulsion system

The engine design is based on the prescribed sea-level static thrust of 80 klbf with a bypass ratio of 9.5 at cruise condition defined by AIRBUS [28]. The requirements that were incorporated into the design were generated by openAD [17] and are shown in Table 4. OpenAD distinguished between different operating conditions, such as take-off, end of field (EOF) and 2nd segment as well as top of climb (TOC) and mid cruise. The CS-25 [30] describes the necessary requirements and considered in openAD. The take-off condition corresponds to break release point with the sea-level static thrust of 80 klbf and the MTOM of 245 t. For EOF, the CS-25.121a is applied, which specifies that the landing gear is extended, no ground effect is included, a required climb gradient is ensured, the aircraft mass is approximately MTOM and the aircraft at lift of speed V_{LOF}. Similarly, the 2nd segment is defined according to CS-25.121b in which the landing gears are retracted and the aircraft accelerated to its second segment speed V_2. For TOC, typical conditions of a minimum rate of climb should be achieved as well as a 0.02 lower Mach number compared to cruise conditions. The mid cruise point is usually not a thrust design point, but rather a point related to efficiency.

Table 4 Engine requirements

Parameter	Unit	Take-off	EOF	2nd segment	TOC	Mid cruise
Delta temp. ISA	K	15	15	15	0	0
Mach number	–	0	0.232	0.232	0.81	0.83
Altitude	ft	0	35	400	33000	36000
Engine rating	–	MTO	RTO	RTO	MCL	MCR
Thrust	klbf	80.0	59.6	64.6	15.8	12.5
Shaft-power offtakes	kW	255	255	255	105	105
Bleed-air offtakes	kg/s	2.901	2.901	2.901	1.160	1.160

Table 5 Engine offtakes offtakes (per Engine)

Parameter	Unit	Take-off/App./ landing	Cruise
Bleed-air offtakes			
w/o Wing anti-ice:	kg/s	1.200	0.990
Wing anti-ice:	kg/s	1.701	0.170
Total:	kg/s	2.901	1.160
Shaft-power offtakes			
Total:	kW	255	105
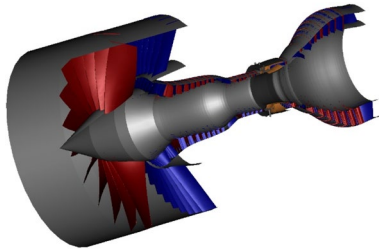
Fig. 14 3D engine geometry

The engine offtakes are estimated by data of the CeRAS CSR-01 open configuration developed by RWTH Aachen [32] and the AVACON aircraft provided by the a project of the German Federal Aviation Research Programme (LuFo) [33]. Table 5 list the engine offtakes, which are based on the CeRAS CSR-01 and AVACON aircraft and are extrapolated in terms of MTOM, PAX and wing span to match with system requirements of the D300-XRF1 aircraft. The differences between take-off as well as approach & landing to the cruise conditions are due to a higher energy demand during lower altitude flight for wing ice protection, lighting, the re- and extraction of landing gear or control surfaces. A distinction is made between the wing anti-icing for the future assessment of a more electric HLFC aircraft using an inductive Wing Ice Protection System (WIPS).

The virtual engine framework GTlab [25] is used for the engine design. A three-spool unmixed high bypass ratio turbofan engine is designed according to the requirements from the overall aircraft design (see Appendix A in Table 4). GTlab predicts the 2D and rough 3D geometry of an engine as shown in Fig. 14) based on thermodynamic cycle data and dimensionless geometry properties of a comparable engine of the same architecture.

The overall pressure ratio is selected as high as possible, considering the maximum compressor section exit temperature at maximum take-off condition and the blade height of the last compressor blade. The bypass ratio of the engine is chosen to match the fan radius according to the geometry of D300-XRF1 nacelle. The fuel-to-air ratio at cruise is selected to limit the temperature at maximum

take-off conditions to its maximum value. The pressure ratio of the fan in the bypass section is selected to fulfill the ideal nozzle velocity condition for unmixed turbofan engines. The speed of shafts is determined by the assumption of circumferential blade velocities at the area averaged radius of the high- and intermediate-pressure compressor. The low spool speed is modeled as a function of the fan pressure ratio in the bypass section. The cooling air demand for the cooled high- and intermediate-pressure turbines is calculated for the maximum take-off condition as a function of the stator inlet temperature and the cooling air temperature. The power offtakes come from the intermediate spool and the customer bleed from the high-pressure compressor after a relative enthalpy change of 0.6. For the turbo component efficiencies, the effect of component size is included by statistical models. For the cooled turbines, also the impact of the cooling air demand on the efficiency is modeled.

Characteristic parameters of the engine design are listed in the Appendix A in Table 12. At cruise (CR) the engine has a thrust specific fuel consumption (tSFC) of 0.51 lb/lbf/hr. The bypass ratio (BPR) is 9.51 and the overall pressure ratio (OPR) reaches 47.0.

The available thrust is limited to minimum and maximum values defined by ratings. In Fig. 15a and b, the operating range of the engine is exemplarily illustrated. In this case, the maximum available thrust corresponds to the maximum climb rating (MCL) and the minimum thrust to the flight idle rating. The ratings are defined by limiter sets to ensure a stable and damage free operation. Between these boundaries defined by the ratings, the deck provides operating points for a continuous operation during the flight.

During the take-off phase of the flight mission, the time limited maximum take-off rating (MTO) is used. Therefore, two decks are provided for the calculation of the flight mission. One that can only be applied during the take-off phase for less than 5 min including operating points between the MTO and idle rating. The other deck is used for continuous operation during climb, cruise, approach and landing. In addition, a separate engine deck is provided for each offtake setting.

5.6 Aircraft performance

In aircraft design, the most dominant factors to meet the TLARs are the wing sizing, i.e., aerodynamics, and the installed thrust [19]. The aircraft mission performance analysis merges the disciplines of aerodynamics, engine design as well as airframe information and provide a measure to compare different aircraft designs. In the following, the aircraft performance at low speed and the cruise mission are presented.
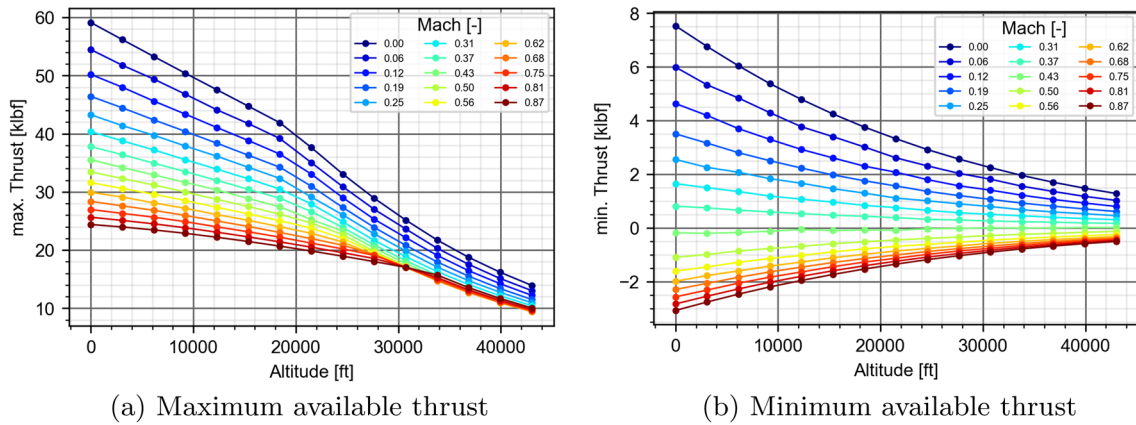
(a) Maximum available thrust   (b) Minimum available thrust

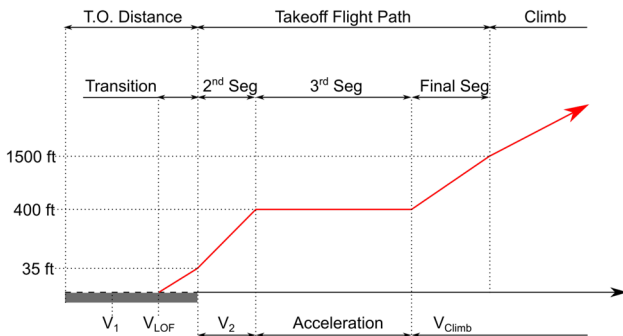**Fig. 15** Available thrust as a function of Mach number in x-direction and flight altitude (flight idle rating)

Fig. 16 Take-off path and definition of segments [26, 27]

Table 6 Take-off properties

Parameter	Unit	Value
Mass	t	245.0
Airport elevation	ft	0
Delta T	°C	0
Runway slope	deg	0
Configuration	–	2220
Take-off distance (AEO)	m	1507
Take-off field length (AEO)	m	1733
Balanced field length	m	2458
Fuel consumption	kg	649.4
V_1 (CAS)	kn	141.7
V_{LOF} (CAS)	kn	150.1
V_2 (CAS)	kn	150.5
$V_{2,min}$ (CAS)	kn	147.3
V_S (CAS)	kn	130.4
$c_{L,max.TO}$ [11]	–	2.325

5.6.1 Low-speed performance

The AEO take-off performance is estimated within the OAD process in particular to estimate the fuel consumption. This information is used for the subsequent mission performance calculation and the synthesis of the higher-fidelity results. The low-speed computation requires additional aircraft information and is listed in Table 6.

The take-off flight path consists of five segments, which are the ground roll segment, the transition segment, the 2nd segment, the 3rd segment and the final segment, as illustrated in Fig. 16. The process is started with break release and accelerates until the lift-off speed is reached. Once the aircraft is airborne, the aircraft continues in the transition segment with the same configuration as during ground roll. Subsequently, the landing gears are retraced for the 2nd segment. The 3rd segment at a constant flight altitude is an acceleration and control surfaced retracting segment. Once the climb speed is reached, the aircraft will climb at constant CAS in its final segment until an altitude of 1500 ft and the end of the take-off flight path. A more detailed description of

the take-off flight path and its different settings is provided by FRÖHLER et al. [26].

The required take-off field length (TOFL) is calculated by finding the longest take-off distance (TOD) for AEO · 1.15, One Engine Inoperative (OEI) or Rejected Take-Off (RTO). The TOFL requirement is determined by the balanced field length (BFL) calculation. The BFL is analyzed by finding the intersection between the OEI and RTO cases as shown Fig. 17. The calculation showed an intersection of OEI and RTO at a BFL = 2458.2 m at a decision speed of V_1 (CAS) = 141.6 kn. Figure 18 shows the sensitivities for a regular operation and analysis the influence of the take-off mass (TOM) and airport pressure altitudes. It indicates that for a higher airport elevation or an increased TOM, the TOFL increases.
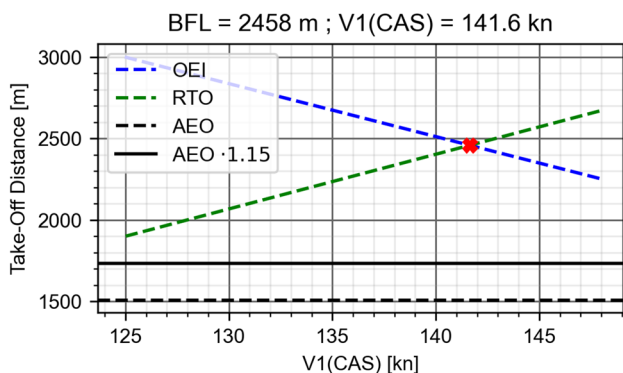
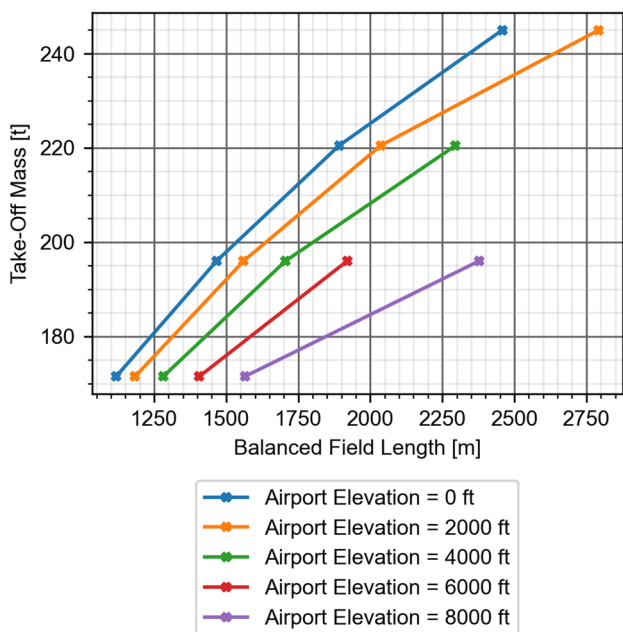**Fig. 17** Balanced field length (BFL) of the D300-XRF1 at SL, ISA condition

Fig. 18 Take-off sensitivities for AEO of the D300-XRF1 at SL, ISA condition

Table 7 Approach & landing properties

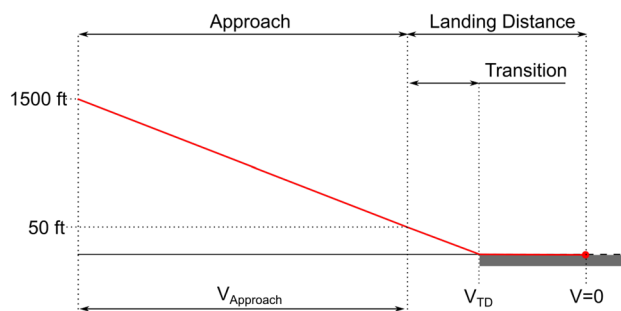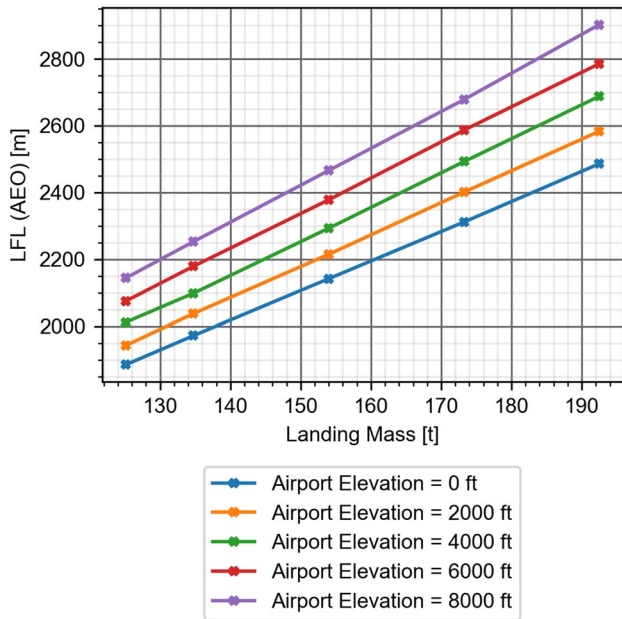| Parameter	Unit	Value
Mass	t	192.5
Airport elevation	ft	0
Delta T	°C	0
Runway slope	deg	0
Configuration	–	2233
Descent flight path angle	deg	– 3
Landing distance	m	1491.6
Landing field length	m	2486
Fuel consumption	kg	145.6
$V_{App.\&L}$ (CAS)	kn	137.0
V_S (CAS)	kn	111.4
$c_{L,maxApp.\&L}$ [11]	–	2.503

Fig. 19 Landing path and definition of various segments [26, 27]

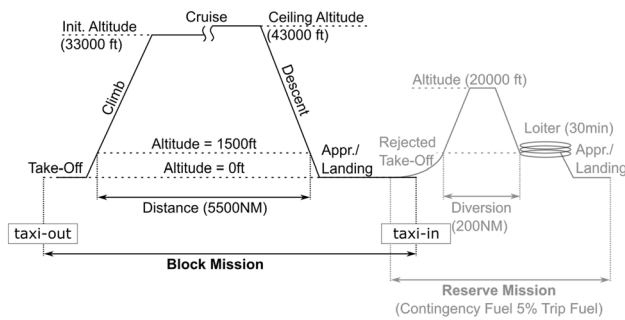adding a safety factor of 1.667 for turbofan engines to the landing distance.

A sensitivity study, shown in Fig. 20, has been performed to analyses the effect of landing mass and aircraft pressure altitude on the landing field length (LFL). The same setting as described in Table 7 has been used for each computation. Results show an increase in LFL with an increase in landing mass and airport elevation.

5.6.2 High-speed performance

The mission performance is analyzed using an AMC which relay on internal mission optimizations based on the specific range, the interaction of aerodynamic and engine performance, and block fuel. Figure 21 illustrates a typical mission profile which is composed out of a block mission segment and a reserve mission segment. The reserve mission is presumed to have a contingency fuel of 5% trip fuel. Therefore, to realize the desired mission range, fuel on board must be sufficient for the block mission segment, a reserve mission segment and the contingency fuel. The trajectory and performance parameter of the design mission are displayed in Appendix A, Fig. 26. The idealized mission performance

The approach & landing performance are analyzed using the described parameter in Table 7. The aircraft is descending with a constant flight path angle of -3°. Furthermore, a constant CAS is prescribed and the aircraft is in landing condition as described in Table 3 with landing gears extended. During approach & landing segment, the D300-XRF1 has a fuel consumption of 145.6 kg.

The trajectory of the approach & landing segment is illustrated in Fig. 19. The approach segment starts at an altitude of 1500 ft and continues to an altitude of 50 ft at a constant flight path angle. The landing distance starts at 50 ft above the airport in which the landing mass of 192.5 t is prescribed. The landing distance continues until the aircraft has come to a complete stop. A required landing field is
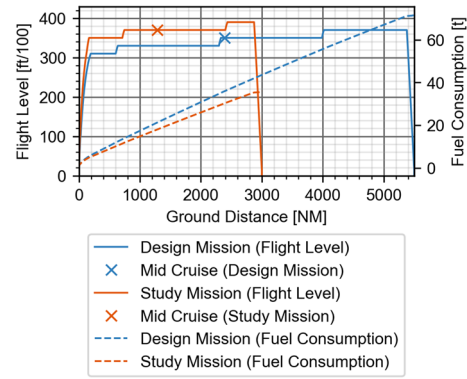
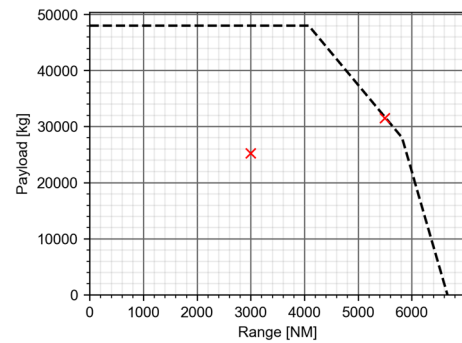**Fig. 20** Landing sensitivities for AEO at ISA conditions for different airport altitudes and landing masses

Fig. 21 Typical mission definition [28]

Fig. 22 Design mission and study trajectory with its fuel consumption

Fig. 23 Payload–range characteristics

is conducted by prescribing a constant CAS of 250 kn for the climb segment until a FL100 is reached. Subsequently, the aircraft accelerates to 300 kn CAS and climbs up to its optimized ICA. A cruise phase with constant Mach number and altitude with a step-climb optimization, based on an optimum specific range, is prescribed. In the decent phase, the aircraft decelerates to 250 kn CAS and is descending to FL100 with constant speed and continues with the approach & landing phase.

A comparison of the mission performance for the design mission and a study mission is shown in Fig. 22. The two missions are distinguished by its range with 5500 NM and 3000 NM and payload with 31.5 t and 25.2 t for the design and study mission, respectively. The cruise Mach number remained constant for both missions. The design mission trajectory differs in terms of ICA and number of cruise steps from the shorter study mission. Due to the shorter range of

the study mission, less fuel is consumed compared to the same distance as the design mission (see dashed lines in Fig. 22). This is explained by the extra mass of fuel to carry the additional fuel for the longer range of the design mission. A summary of the mission phases with its flight time, fuel mass and distance is listed in the Appendix A, Table 13 and Table 14. As illustrated in Fig. 21, the mission is divided into two sections, the block mission and the reserve mission. For the aircraft performance, the necessary fuel on board has to be sufficient for both block and reserve mission with the additional contingency fuel in case of an emergency. For the block mission, a fuel consumption of 71.8 t with a total flight time of 721.5 min for its design range of 5500 NM. The reserve mission considers a 200 NM range mission and a 30 min holding phase which resulted in a total of 321 NM range and 9.6 t of fuel consumption which includes the additional contingency fuel with 5% of block fuel.

The payload–range characteristics are displayed in Fig. 23. The maximum payload is prescribed to 48 t, with a design passenger capacity of 300 PAX at 105 kg/PAX and additional cargo of 16.5 t. With a maximum payload, the range is estimated to be 4080.6 NM. The range is extended by reducing the payload and constant fuel mass on the

condition that the MTOM is not exceeded. The design mission is defined at full passenger load resulting to a range of 5500 NM. Subsequently, the payload is reduced, while fuel is increased until the max. fuel volume is reached at the max. range of 5818.5 NM. To further increase the range at constant fuel mass, the payload is reduced. This results in the ferry range of 6664.5 NM.

5.7 Direct operating cost

The direct operating costs (DOC) are estimated according to a method proposed by THORBECK [34]. Using the method, the DOCs are divided into energy costs, fees for airport services and air traffic control (ATC), maintenance, crew and capital, which depend on the aircraft characteristics and fuel price. DOCs per year depend on the number of passengers and the distance traveled, which are then summarized as available seat kilometers (ASK) per year. For the design of the D300-XRF1, a year entry into service in 2010 is assumed. Therefore, an average fuel price in the year 2010 of 67.72 € / US-Barrel [35] will be used as a reference for the fuel price. The Flight cycles per year are estimated at 2749 hours of annual forced downtime.

The aviation industry is highly cost driven, and when new technologies are introduced, the change in profitability could be a potential inhibitor on the one hand and a driver of the development on the other. Figure 24a and b shows the DOCs for the design mission and study mission of the D300-XRF1. For the design mission, with a range of 5500 NM

and a passenger capacity of 300 PAX, the highest cost is the jet fuel with 35% and 30% for the capital cost. The DOC amounts to 3.56 USD 2010 per 100 ASK, which is lower compared to the study mission with 4.8 USD$_{2010}$/100ASK. The difference results from the larger proportion of airport fees and the number cycles for the study mission with a lower range of 3000 NM.

6 Conclusion

This paper presents the development of a medium to long-haul reference aircraft. For the development of new technologies, a reference aircraft with a certain level of detail must be defined in order to have a thorough assessment. For this purpose, AIRBUS provided the XRF1 as a reference aircraft.

In the current paper, the XRF1 reference aircraft designed by DLR is presented, namely the D300-XRF1. The aircraft design was based on the same TLARs as provided by the AIRBUS XRF1 mini database [28]. In addition, two DLR internal projects [8, 14] are identified, which supports the development of the XRF1 aircraft and serves as a basis for the design presented in this study. These projects considered the overall aircraft design and provided a detailed aircraft geometry description as well as high-fidelity data of aerodynamic polars and the mass breakdown with the corresponding material selection. For the development of the D300-XRF1, an OAD process was created using the conceptual aircraft design tool openAD and higher-fidelity disciplinary
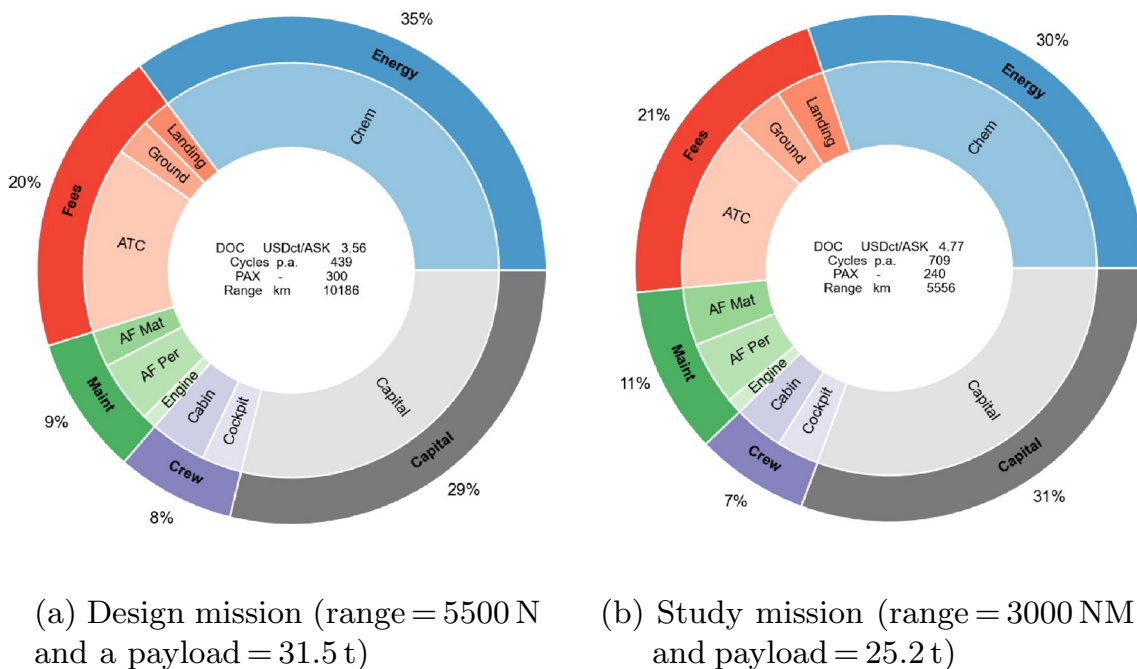

(a) Design mission (range = 5500 N and a payload = 31.5 t)

(b) Study mission (range = 3000 NM and payload = 25.2 t)

Fig. 24 Direct operating costs (DOC)

tools were linked. Results of the aircraft geometry, mass estimations, aerodynamics, engine performance, and mission performance were shown.

For future studies, the reference aircraft is used to compare new technologies. Starting from the reference D300-XRF1, a baseline configuration should be developed for the next steps in evaluating new technologies with a corresponding year in entry into service and incremental technology improvements. Once the baseline configuration is established, the new technologies be analyzed in detail. For this, each developed component is integrated into the baseline aircraft to investigate the effect of each component separately. This provides a detail assessment of novel technologies and futuristic aircraft with a consistent reference model.

Appendix A additional data of the D300-XRF1
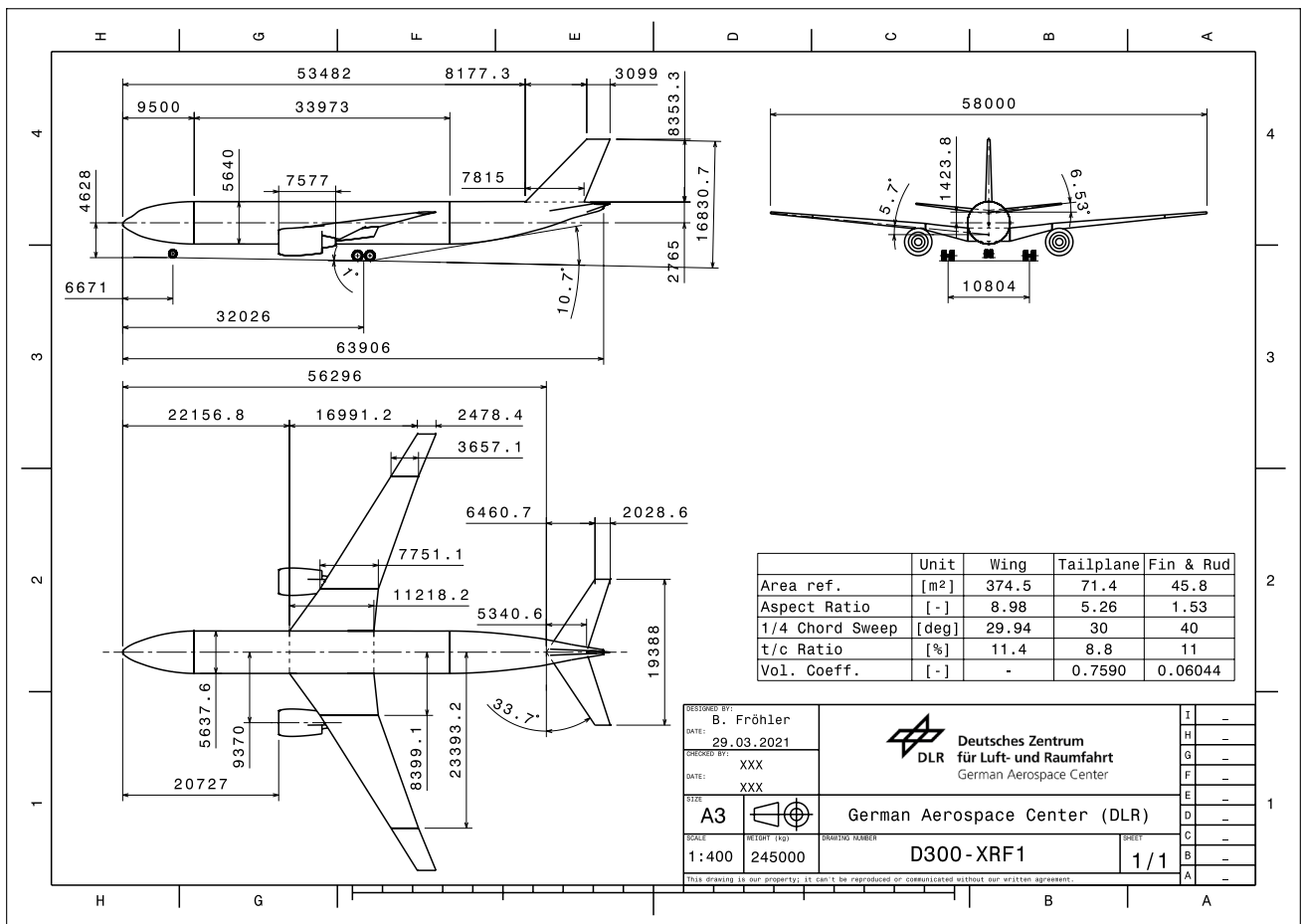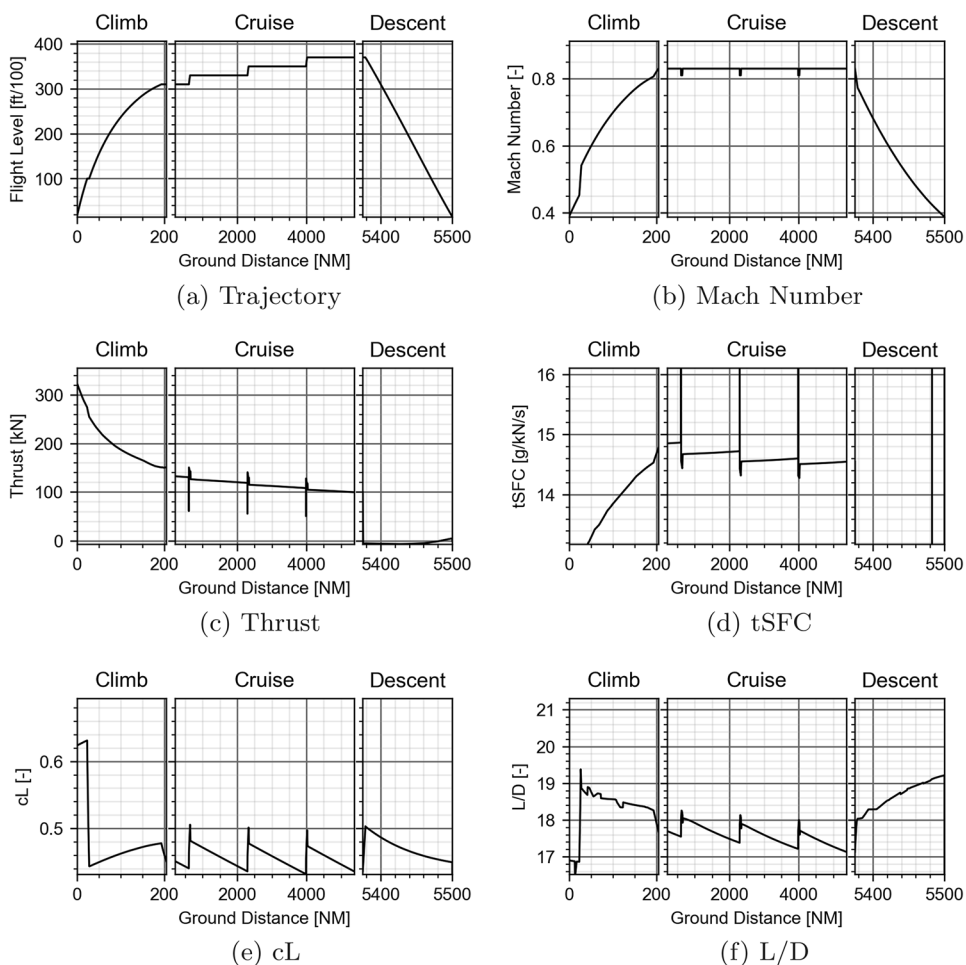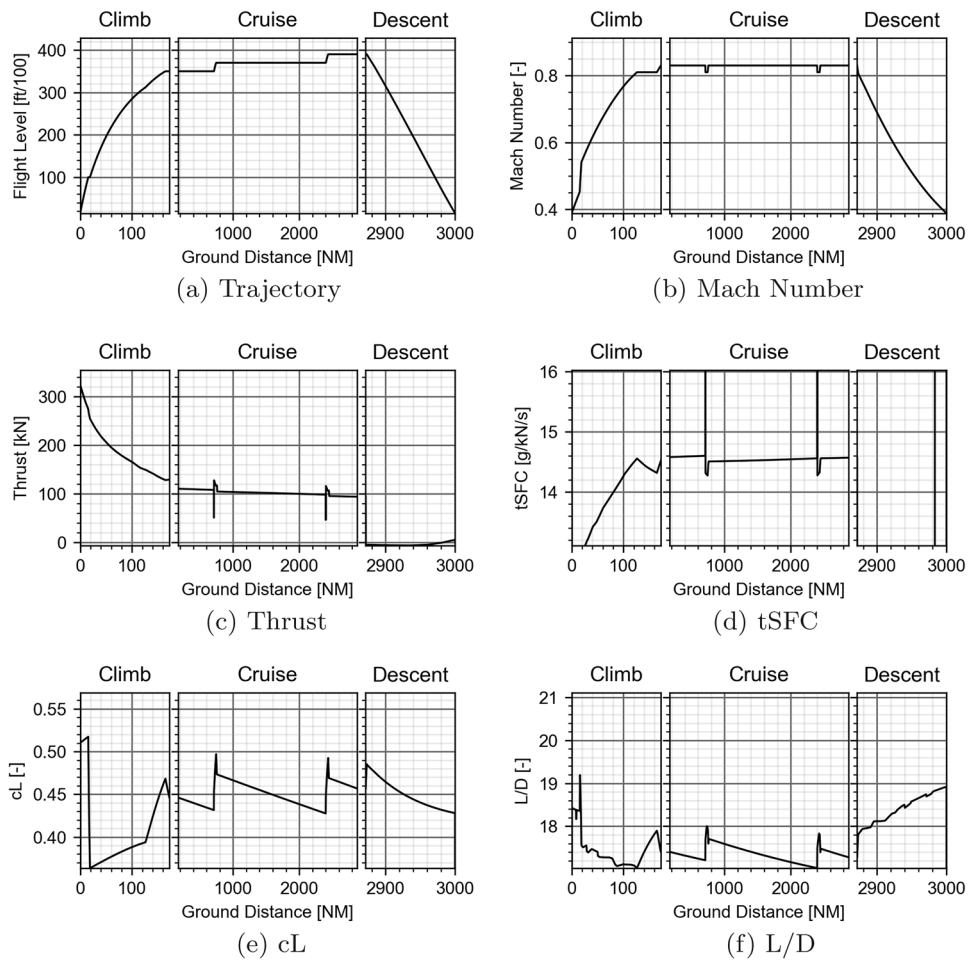
See Figs. 25, 26, 27 and Tables 8, 9, 10, 11, 12, 13, 14.

Fig. 25 Detailed three-view of the D300-XRF1

Fig. 26 Design mission performance (Range = 5500 NM and Payload = 31.5 t)

(a) Trajectory

(b) Mach Number

(c) Thrust

(d) tSFC

(e) cL

(f) L/D

Fig. 27 Study mission performance (Range = 3000 NM and Payload = 25.2 t)

(a) Trajectory

(b) Mach Number

(c) Thrust

(d) tSFC

(e) cL

(f) L/D

Table 8 D300-XRF1 overall mass properties

Component	Mass [kg]
Wing	34240
Fuselage structure	25806
HTP	2018
VTP	1253
Pylons	3377
Power units	18379
Main gear	8882
Nose gear	843
Systems	10734
Furnishings	8231
Manufacturer empty mass	113762
Operating items (PAPP2007 typical layout)	18731
Operating empty mass	132500
Maximum payload	48000
Maximum fuel	84500
Maximum zero-fuel mass	180500
Maximum landing mass	192500
Maximum take-off mass	245000

Table 9 D300-XRF1 system mass breakdown

Component	Mass [kg]
Air conditioning	1677
Auxiliary power unit (APU)	428
Automatic flight system	77
Communication system	597
De-icing	54
Electrical system	3004
Flight controls	1992
Fire protection	287
Hydraulic system	2000
Instrument panels	30
Navigation	587
Miscellaneous	0

Table 10 D300-XRF1 wing mass breakdown

Component	Mass [kg]
Wing box	24171
Ribs	(3617)
Shell	(16555)
Spars	(3999)
Fixed leading edge	1412
Fixed trailing edge	2634
Movable leading edge	1430
Slats	(1430)
Movable trailing edge	2153
Flaps	(1543)
Aileron	(332)
Spoilers	(278)
Pylon attachments	429
Landing gear support	1215
Miscellaneous	796
Total wing	34240

Table 11 D300-XRF1 Operator's Items (3-Class Layout) mass breakdown

Component	Mass [kg]
Seat mounted electronical system	182
Unusable fuel	436
A/C documents and tool Kit	29
Galley structures	2471
Passenger seats	7422
Fluid for toilets	54
Emergency equipment	559
Catering	3979
Water for galleys and toilets	1022
Engine and APU Oil	111
Crew	835
Crew rest	1632
Operating items	18732

Table 12 Description of the thermodynamic engine design

Parameter	Unit	MDP	TOC	MTO-SLS-MAX	MTO-SLS-MAX-0	EOF	2nd Segment
Mass flow	kg/s	491.8	563.3	1227.3	1259.2	1179.9	1196.3
Mach No	–	0.83	0.81	0.0	0.0	0.232	0.232
Altitude	m	10972.8	10058.4	0.0	0.0	11.7	121.9
Fan inlet	–	0.625	0.654	0.599	0.599	0.536	0.557
Thrust	lbf	12.6	15.8	80.0	80.0	52.1	54.8
tSFC	lb/lbf/hr	0.511	0.510	0.282	0.272	0.364	0.364
OPR	–	46.97	50.29	48.62	48.76	41.50	43.59
BPR	–	9.51	9.22	8.98	8.97	9.54	9.4

Table 13 Description of the design mission performance with all engine operating

Mission phase	Flight time [min]	Fuel mass [kg]	Distance [NM]
Block mission	721.5	71830.6	5500
Taxi-out	9	339.4	0
Take-off	2	649.7	0
Climb	31.0	5147.9	204.6
Cruise	646.8	64981.0	5148.9
Descent	22.6	378.6	124.9
Approach & landing	5	145.6	0
(Taxi-In)	(5)	(188.6)	(0)
Reserve mission	71.1	9584.3	321.1
Go-Around	1.6	584.7	0
Diversion climb	7.4	1448.5	43.4
Diversion cruise	13.7	1222.4	89.0
Diversion descent	14.2	308.2	69.4
Holding	30	2324.4	119.3
Diversion approach & Landing	4.5	131.0	0
Contingency	0	3565.1	0

Table 14 Description of the study mission performance with all engine operating

Mission phase	Flight time [min]	Fuel mass [kg]	Distance [NM]
Block mission	409.4	36045.1	3000
Taxi-out	9.0	339.4	0.0
Take-off	2.0	649.4	0.0
Climb	25.3	3977.2	172.2
Cruise	340.1	30367.3	2699.0
Descent	23.0	377.6	128.8
Approach & landing	5.0	145.5	0.0
(Taxi-In)	5.0	188.6	0.0
Reserve mission	70.7	9967.8	311
Go-around	1.6	584.5	0.0
Diversion climb	7.0	1358.5	40.7
Diversion cruise	13.9	1253.7	92.8
Diversion descent	14.0	303.7	68.3
Holding	30.0	2211.5	119.3
Diversion approach & landing	4.5	131.0	0.0
Contingency	0.0	1775.9	0.0

Declarations

Conflict of interest The authors have no competing interests to declare that are relevant to the content of this article.

References

1. Lefebvre, T., Schmollgruber, P., Blondeau, C., Carrier, G.: Aircraft conceptual design in a multi-level, multi-fidelity, multi-disciplinary optimization process. ICAS (2012)
2. Rosenblum, J.P., et al.: Active flow separation control at the outer wing. CEAS Aeronaut. J. **11**(4), 823–836 (2019). https://doi.org/10.1007/s13272-019-00402-4
3. Meheut, M.: Multidisciplinary Adjoint-based optimizations in the MADELEINE project: overview and main results. American Institute of Aeronautics and Astronautics (2021)
4. Krüger, W.R., König, J.: Editorial for the CEAS aeronautical journal special edition on smart fixed wing aircraft, WP 1.2 load control. CEAS Aeronaut. J. **10**(4), 975–976 (2019). https://doi.org/10.1007/s13272-019-00418-w
5. Krüger, W.R., Dillinger, J., Breuker, R.D., Haydn, K.: Investigations of passive wing technologies for load reduction. CEAS Aeronaut. J. **10**(4), 977–993 (2019). https://doi.org/10.1007/s13272-019-00393-2
6. Schulze, M., Hecken, T., Ritter, M., Klimmek, T.: AEROGUST; aeroelasticgust modelling; d2.14 report on simultaneous gust and control surface deflection (project no: 636053). Tech. Rep., Deutsches Zentrum für Luft- und Raumfahrt e.V (2018)
7. Jepsen, J., Nagel, B.: Digital-x, meilensteinbericht 4.3.3. Tech. Rep., Deutsches Zentrum für Luft- und Raumfahrt e.V (2013)
8. Görtz, S., Krumbein, A., Ritter, M.: & Hofmann, J. Wissenschaftlicher ergebnisbericht. Tech. Rep., Deutsches Zentrum für Luft- und Raumfahrt e.V, VicToria (2020)
9. Görtz, S., et al.: Overview of collaborative multi-fidelity multidisciplinary design optimization activities in the DLR project VicToria. American Institute of Aeronautics and Astronautics (2020)
10. Abu-Zurayk, M., et al.: Sensitivity-based multifidelity multidisciplinary optimization of a powered aircraft subject to a comprehensive set of loads. American Institute of Aeronautics and Astronautics (2020)
11. Bertram, O.: Neue Entwurfsmethoden Zukünftiger Steuerflächenkonzepte: (im LuFo V-2 Con.Move-Verbundprojekt). Tech. Rep., Deutsches Zentrum für Luft- und Raumfahrt e.V (2020)
12. Schültke, F., Aigner, B., Effing, T., Strathoff, P., Stumpf, E.: MICADO overview of recent developments within the conceptual aircraft design and optimization environment. Deutsche Gesellschaft für Luft- und Raumfahrt - Lilienthal-Oberth eV (2021). https://doi.org/10.25967/530093
13. Krengel, M. D.: MICADO Design of XRF1 V3: Technical Report. Tech. Rep., Deutsches Zentrum für Luft- und Raumfahrt e.V (2019)
14. Wild, J.: XRF1 - highlift design documentation. Tech. Rep., Deutsches Zentrum für Luft- und Raumfahrt e.V (2019)
15. Seider, D., Fischer, P.M., Litz, M., Schreiber, A., Gerndt, A.: Open source software framework for applications in aeronautics and space. IEEE (2012)
16. Alder, M., Moerland, E., Jepsen, J., Nagel, B.: Recent advances in establishing a common language for aircraft design with cpacs (2020). https://elib.dlr.de/134341/
17. Wöhler, S., Atanasov, G., Silberhorn, D., Fröhler, B., Zill, T.: Preliminary aircraft design within a multidisciplinary and multifidelity design environment. *Aerospace Europe Conference 2020* (2020)
18. Torenbeek, E.: Synthesis of subsonic airplane design. Springer Netherlands (2013)
19. Torenbeek, E.: Advanced aircraft design: conceptual design, technology and optimization of subsonic civil airplanes, 1st edn. Wiley (2013)
20. Roskam, J.: Airplane Design, Parts 1–8. In: Design Analysis & Research, 2nd edn. Wiley (1989)
21. Raymer, D.P.: Aircraft design: a conceptual approach (AIAA education series), 6th edn. American Institute of Aeronautics & Astronautics (2018)
22. Jenkinson, L.R., Simpkin, P., Rhodes, D.: Civil jet aircraft design. Elsevier Science & Technology (1999)
23. Bräunling, W.J.G.: Flugzeugtriebwerke. Springer-Verlag GmbH (2015)
24. Horstmann, K. H.: Ein mehrfach-traglinienverfahren und seine verwendung für entwurf und nachrechnung nichtplanarer flügelanordnungen. Tech. Rep., Deutsches Zentrum für Luft- und Raumfahrt e.V (1987)
25. Reitenbach, S., et al.: Collaborative aircraft engine preliminary design using a virtual engine platform part a: architecture and methodology. American Institute of Aeronautics and Astronautics (2020)
26. Fröhler, B., Hesse, C., Atanasov, G., Wassink, P.: Disciplinary sub-processes to assess low-speed performance and noise characterisics within an aircraft design environment. Deutscher Luft- und Raumfahrtkongress 2020 (2021). https://doi.org/10.25967/530201
27. AIRBUS. Flight Operations Support & Line Assistance; getting to grips with aircraft performance. https://www.smartcockpit.com/docs/getting-to-grips-to-aircraft-noise.pdf (2002). Accessed 18 May 2022
28. Marr, I.: XRF1 aircraft: mini - data basis for design (DBD) live document for updating. Tech. Rep, AIRBUS (2020)
29. Walther, J.-N., Hesse, C., Biedermann, J., Nagel, B.: High fidelity digital cabin mock-up based on preliminary aircraft design data for virtual reality applications and beyond. American Institute of Aeronautics and Astronautics (2021)
30. European Aviation Safety Agency. Certification specifications for large aeroplanes CS-25. https://www.easa.europa.eu/downloads/134259/en (2007). Accessed 18 May 2022
31. Vassberg, J., Dehaan, M., Rivers, M., Wahls, R.: Development of a common research model for applied CFD validation studies. American Institute of Aeronautics and Astronautics, Rome (2008)
32. RWTH-Aachen.: Ceras central reference aircraft data system. https://ceras.ilr.rwth-aachen.de/ (2022). Accessed 20 Apr 2022
33. Wöhler, S., Hartmann, J., Prenzel, E., Kwik, H.: Preliminary aircraft design for a midrange reference aircraft taking advanced technologies into account as part of the avacon project for an entry into service in 2028 (2019)
34. Thorbeck, J.: From aircraft performance to aircraft assessment. Tech. Rep., DGLR Short Course: Aircraft Design, 2007, Berlin (2007)
35. U.S. Energy Information Administration (eia).: U.S. gulf coast kerosene-type jet fuel spot price fob (dollars per gallon). https://www.eia.gov/dnav/pet/hist/EER_EPJK_PF4_RGC_DPGD.htm (2022). Accessed 20 Apr 2022